Research Article

Inhibitor of DNA binding 2 accelerates nerve regeneration after sciatic nerve injury in mice

https://doi.org/10.4103/1673-5374.313054

Date of submission: September 15, 2020

Date of decision: November 11, 2020

Date of acceptance: January 30, 2021

Date of web publication: April 23, 2021

Zhong-Hai Huang[1], Ai-Ying Feng[1], Jing Liu[1], Libing Zhou[1], Bing Zhou[2,*], Panpan Yu[1,*]

Graphical Abstract *Id2 accelerates axonal regeneration, promotes neuromuscular reinnervation and enhances functional improvement after sciatic nerve injury*

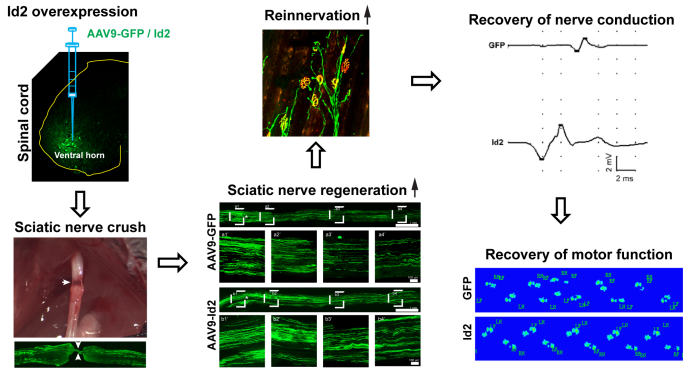

Abstract

Inhibitor of DNA binding 2 (Id2) can promote axonal regeneration after injury of the central nervous system. However, whether Id2 can promote axonal regeneration and functional recovery after peripheral nerve injury is currently unknown. In this study, we established a mouse model of bilateral sciatic nerve crush injury. Two weeks before injury, AAV9-Id2-3×Flag-GFP was injected stereotaxically into the bilateral ventral horn of lumbar spinal cord. Our results showed that Id2 was successfully delivered into spinal cord motor neurons projecting to the sciatic nerve, and the number of regenerated motor axons in the sciatic nerve distal to the crush site was increased at 2 weeks after injury, arriving at the tibial nerve and reinnervating a few endplates in the gastrocnemius muscle. By 1 month after injury, extensive neuromuscular reinnervation occurred. In addition, the amplitude of compound muscle action potentials of the gastrocnemius muscle was markedly recovered, and their latency was shortened. These findings suggest that Id2 can accelerate axonal regeneration, promote neuromuscular reinnervation, and enhance functional improvement following sciatic nerve injury. Therefore, elevating the level of Id2 in adult neurons may present a promising strategy for peripheral nerve repair following injury. The study was approved by the Experimental Animal Ethics Committee of Jinan University (approval No. 20160302003) on March 2, 2016.

Key Words: axonal regeneration; functional recovery; inhibitor of DNA binding 2; motor neuron; neuromuscular junctions; peripheral nerve; reinnervation; sciatic nerve injury

Chinese Library Classification No. R456; R745; R364.3+3

Introduction

Although adult peripheral nerves retain considerable regenerative capabilities after injury, functional outcomes often remain incomplete in patients (Fu and Gordon, 1995; Sulaiman and Gordon, 2013; Panagopoulos et al., 2017). This is especially the case after damage of large nerve trunks far from their targets. For patients with sciatic nerve injury at the hip level or brachial plexus injury at the shoulder level, outcomes are usually poor and complete functional recovery is seldom achieved (Sulaiman and Gordon, 2013). In both cases, injured axons are required to regenerate over a long distance (as much as 1 m) to reinnervate their target muscles in the hand and foot. This regeneration and reinnervation process can take several months or even several years (Sulaiman and Gordon, 2013). During the prolonged period of chronic denervation, muscle fibers undergo atrophy and degeneration leading to irreversible loss of function and strength. Therefore, efforts to accelerate the rate of axonal regeneration and thus shorten the duration of the reinnervation process may be a useful way to improve functional recovery and prevent the occurrence of substantial muscle atrophy after peripheral nerve injury (Gaudet et al., 2011; Jiang et al., 2020; Tang, 2020).

[1]Guangdong-Hong Kong-Macau Institute of Central Nervous System Regeneration; Ministry of Education Joint International Research Laboratory of Central Nervous System Regeneration, Jinan University, Guangzhou, Guangdong Province, China; [2]Interdisciplinary Innovation Institute of Medicine and Engineering, Beijing Advanced Innovation Center for Big Data-Based Precision Medicine, Beihang University, Beijing, China

*Correspondence to: Panpan Yu, PhD, yupanpan21@jnu.edu.cn; Bing Zhou, PhD, bingzh@buaa.edu.cn.

https://orcid.org/0000-0002-4479-1479 (Panpan Yu); https://orcid.org/0000-0002-7718-2311 (Bing Zhou)

Funding: *This work was supported by the National Natural Science Foundation of China, Nos. 82071369 (to PY) and 81971198 (to BZ); Guangdong grant 'Key Technologies for Treatment of Brain Disorders' of China, No. 2018B030332001 (to LZ and PY); Guangzhou Key Projects of Brain Science and Brain-Like Intelligence Technology, China, No. 20200730090 (to LZ); the Natural Science Foundation of Beijing of China, No. 7192103 (to BZ); and the Clinical Innovation Research Program of Guangzhou Regenerative Medicine and Health Guangdong Laboratory of China, No. 2018GZR0201006 (to PY).*

How to cite this article: *Huang ZH, Feng AY, Liu J, Zhou L, Zhou B, Yu P (2021) Inhibitor of DNA binding 2 accelerates nerve regeneration after sciatic nerve injury in mice. Neural Regen Res 16(12):2542-2548.*

Inhibitor of DNA binding 2 (Id2) is a negative regulator of basic helix-loop-helix transcription factors (Benezra et al., 1990). Expression of Id2 in neurons is developmentally downregulated, correlating with the loss of intrinsic regenerative ability of neurons in the central nervous system (CNS) during neuronal maturation (Tzeng and de Vellis, 1998; Lasorella et al., 2006; Ko et al., 2016). We previously found that Id2 overexpression in adult dorsal root ganglion neurons and embryonic cortical neurons *in vitro* dramatically promoted axonal growth (Yu et al., 2011; Huang et al., 2019). After spinal cord dorsal hemisection in mice, Id2 significantly attenuated the axonal dying back of ascending sensory axons in the dorsal column following axotomy (Yu et al., 2011). However, the promoting effect of Id2 on axonal regeneration after spinal cord injury *in vivo* was relatively mild, with only a few fibers extending into the lesion and no axons transversing the lesion (Yu et al., 2011). This may have resulted from the hostile environment within the spinal cord lesion site, which contains numerous inhibitors of axonal regeneration such as myelin-associated inhibitors and chondroitin sulfate proteoglycans (Yiu and He, 2006; Fitch and Silver, 2008). In contrast to the CNS, the local microenvironment of the peripheral nerve system (PNS) is favorable for nerve regrowth (Huebner and Strittmatter, 2009; Toy and Namgung, 2013). Therefore, Id2 is expected to exhibit a more prominent promoting effect on axonal regeneration in the PNS compared with the CNS. In this study, we investigated the effect of Id2 on motor axonal regeneration and functional recovery using a complete sciatic nerve crush injury model in mice.

Materials and Methods

AAV9-Id2 preparation

AAV9-Id2 packaging services were provided by Vigene Bioscience (Jinan, China). The mouse Id2 sequence (NM_010496) with a C-terminal 3×Flag tag was synthetized and inserted into the pAV-CMV-P2A-GFP vector, which separately expresses an Id2-3×Flag fusion protein and green fluorescent protein (GFP) reporter (Vigene Bioscience).

Animals

Adult female C57BL/6 mice (*n* = 37, aged 8–9 weeks) were purchased from Guangdong Laboratory Animals Center, China (License No. SCXK (Yue) 2013-0002) and housed in a light- and temperature-controlled room with ad libitum access to food and water. All animal experiments were approved by the Experimental Animal Ethics Committee of Jinan University (approval No. 20160302003) on March 2, 2016. Surgical procedures and postoperative animal care were conducted in accordance with the Guide for the Care and Use of Laboratory Animals (National Research Council, 1996, USA). All experiments were designed and reported according to Animal Research: Reporting of *In Vivo* Experiments (ARRIVE) guidelines. In total, 32 mice were randomly divided into GFP (Control; *n* = 16) and Id2 (AAV9-Id2; *n* = 16) groups. Five animals from each group were used for confirmation of AAV9 expression and characterization of the sciatic nerve crush injury model. Six animals from each group were used for measurements of axonal regeneration 2 weeks after injury. Five animals from each group were used for evaluations of electrophysiological function, motor function, and neuromuscular reinnervation at 1 month after injury. An additional five normal mice were used for electrophysiological analysis as uninjured controls.

Intraspinal injection of AAV9 virus

Under deep anesthesia with intraperitoneal injection of 1.25% avertin at a dosage of 20 mL/kg body weight, the T13 thoracic vertebra (corresponding to L4 and L5 spinal nerve origin points) were exposed and immobilized on a mouse vertebral-stabilizing device, as previously described (Zhang et al., 2013; Wu et al., 2019). Laminectomy was performed to expose the spinal cord. AAV9-Id2-3×Flag-GFP or AAV9-GFP virus (Vigene Bioscience) at a titer of 6×10^{12} viral genomes/mL was injected stereotaxically into the bilateral ventral horn using a glass micropipette attached to a Hamilton syringe. Entry points into the spinal cord were 0.4 mm lateral to the midline bilaterally, with injections into the ventral spinal cord at a depth of 1.0 mm. For each animal, a total of four sites were injected, two in the right ventral horn and two in the left ventral horn. For each site, 0.5 µL of AAV9 virus were administrated slowly within 2 minutes, and the glass micropipette remained in position for an additional 5 minutes to prevent solution leakage. After injection, the muscles and skin were sutured in layers, and mice were allowed to recover on a heating pad at 37°C. To prevent dehydration, 1 mL of saline was injected subcutaneously.

Sciatic nerve crush

Two weeks after AAV9 injection, mice were subjected to bilateral sciatic nerve crush injury, which was conducted as previously described with some modifications (Zhou et al., 2016; Li et al., 2019). Under anesthesia with intraperitoneal injection of 1.25% avertin at a dosage of 20 mL/kg body weight, a longitudinal incision was made along the lateral thigh to expose the sciatic nerve. After gently separating the sciatic nerve from the surrounding connective tissue, it was crushed at a position 1 cm proximal to its trifurcation with a No. 5 fine forceps (Fine Science Tools, Foster City, CA, USA) for 30 seconds. The crush site was marked using a 9-0 nylon suture. The muscles and skin were sutured in layers, and animals were subsequently placed on a heating pad at 37°C until they recovered from anesthesia.

Histology

At 1 hour, 2 weeks, and 1 month after sciatic nerve crush, animals were transcardially perfused with phosphate-buffered saline (PBS, pH 7.4) followed by ice-cold 4% paraformaldehyde in PBS. Spinal cords, sciatic nerves, and gastrocnemius muscles were collected. After post-fixation, samples were immersed in 20% sucrose solution, followed by 30% sucrose solution until they sank. Lumbar spinal cord segments containing the injection sites were cryosectioned transversely at a thickness of 20 µm. Serial sections of sciatic nerve segments were cut longitudinally at a thickness of 12 µm. Serial longitudinal sections of gastrocnemius muscles were prepared at a thickness of 40 µm.

Characterization of AAV9 expression

To characterize AAV9 expression, spinal cord sections were immunostained with chicken anti-GFP (1:1000; Abcam, Cambridge, UK), goat anti-choline acetyltransferase (ChAT; 1:200, Millipore, Burlington, MA, USA) antibodies, or with chicken anti-GFP (1:1000) and mouse anti-Flag (1:500; Sigma, St. Louis, MO, USA) antibodies. The following secondary antibodies were used: Alexa Fluor 488-conjugated donkey anti-chicken IgG, Alexa Fluor 546-conjugated donkey anti-goat IgG, and Alexa Fluor 546-conjugated donkey anti-mouse IgG (all 1:1000; Thermo Fisher Scientific, Waltham, MA, USA). Images were obtained with an Imager Z2 microscope or LSM700 confocal microscope (both from Zeiss, Jena, Germany).

Measurement of axonal regeneration

A set of sciatic nerve sections from each sciatic nerve sample were stained with chicken anti-GFP antibody (1:1000), and

images were acquired using an Imager Z2 microscope with a 20× objective. Numbers of axons were counted in the segment 1 mm proximal to the injury site (0 mm), as well as segments 1.0, 2.0, 3.0, and 9 mm distal; distal counts were normalized to counts observed 1 mm proximal to the injury site. The regeneration index is presented as a percentage of axons at each position to the number observed 1 mm proximal to the injury site. To analyze GFP^+ axons in the tibial nerve extending into the gastrocnemius muscles, four to six sections from each sample were counted and average numbers of GFP^+ fibers per section were calculated.

Motor endplate evaluation

A set of sections (spaced 200 μm apart) of gastrocnemius muscles were stained with chicken anti-GFP (1:1000) and Alexa Flour 594-conjugated α-bungarotoxin (1:1000, Cat# B13423, Molecular Probes, Eugene, OR, USA) to label motor endplates. Tiled images of individual whole gastrocnemius muscle sections were obtained using an Imager Z2 microscope with 20× objective. Numbers of fully innervated (entire endplate covered by a GFP^+ axon terminus) and partially innervated (not fully innervated by a GFP^+ axon terminus) endplates within each section were counted. Total numbers of fully innervated and partially innervated endplates for each animal were calculated by adding numbers observed for each set of sections.

Catwalk gait analysis

Before sciatic nerve injury and 1 month after injury, motor function was evaluated with a Catwalk gait analysis system (CatWalk XT 9.1, Noldus Information Technology, Wageningen, Netherlands). Mice were habituated to the system for 3 consecutive days before the experiment started. Footprints were captured as each mouse voluntarily traversed a glass plate towards a goal box. CatWalk XT visualizes the prints and calculates parameters related to print dimensions, as well as time and distance relationships between footfalls (Bozkurt et al., 2008). Three walking paths were recorded for each animal. The following parameters of hind paws were analyzed: print area, base of support (distance between the two hind paws), and stride length.

Electrophysiological function assessment

For characterization of our sciatic nerve crush injury model, complete interruption of neuromuscular transduction was confirmed electrophysiologically before and 1 day after crush. Electrophysiological functional recovery was assessed 1 month after sciatic nerve injury. Compound muscle action potentials we recorded from the gastrocnemius muscle following electrical stimulation of the proximal sciatic nerve using a Nicolet EDX Viking Quest EMG System (Natus, Pleasanton, CA, USA). Both sides of each animal were recorded. Briefly, following anesthesia with propofol (30 μL/g), the sciatic nerve of mice was exposed and a stimulating electrode was inserted into the sciatic nerve 3 mm proximal to the crush site. In addition, a pair of recording electrodes was inserted into the gastrocnemius muscle to record compound muscle action potentials with a Keypoint Portable (Dantec Biomed, Skovlunde, Denmark). Amplitude and latency were defined to determine the strength and speed of nerve conduction.

Statistical analysis

GraphPad Prism 6 (GraphPad, San Diego, CA, USA) was used to generate graphics and for statistical analysis. Data are presented as mean ± standard error of mean (SEM) or mean ± standard deviation (SD), as indicated in each figure legend. Two-tailed Student's *t*-test is applied to compare differences between two groups. One-way or two-way analysis of variance followed by Tukey's or Bonferroni's *post hoc* test was applied for multiple comparisons. Differences were considered statistically significant at $P < 0.05$.

Results

Characterization of Id2 expression in motor neurons and establishment of sciatic nerve crush model for evaluating motor axonal regeneration

Two weeks after intraspinal microinjection of AAV9-GFP or AAV9-Id2 into the spinal ventral horn of the lumbar segment, co-labeling of ChAT-positive motor neurons with GFP was observed in both GFP and Id2 groups (**Figure 1A** and **B**). Expression of Id2-Flag fusion protein in infected neurons was confirmed by staining with an anti-Flag antibody (**Figure 1C**). Overall infection efficiencies of AAV9-GFP and AAV9-Id2 were comparable ($P > 0.05$), with over 80% of motor neurons ($ChAT^+$) labeled by GFP at the injection center (**Figure 1D**). Axons of these motor neurons projecting to the sciatic nerve were also labeled by GFP (**Figure 1E**), enabling assessment of sciatic nerve regeneration following injury. The crush site readily became transparent after sciatic nerve crush and nerve continuity was completely interrupted, while the epineurium of the nerve remained continuous (**Figure 1F**). Complete interruption of axons was further verified histologically and electrophysiologically. All GFP^+ axons were disrupted at the injury site with no axon sparing observed (**Figure 1G**). Evoked compound muscle action potentials following stimulation of sciatic nerve disappeared when recorded 1 day after crush (**Figure 1H**).

Overexpression of Id2 accelerates the rate of nerve regeneration after sciatic nerve crush

To assess axonal regeneration after sciatic nerve injury, numbers of GFP^+ axons projecting from motor neurons in the lumbar spinal cord were quantified at various distances from the crush site (**Figure 2**). As peripheral nerves retain considerable regenerative capacity, many GFP^+ axons were found to extend beyond the crush site in both GFP and Id2 groups 2 weeks after sciatic nerve crush. Numbers of GFP^+ axons were comparable at the injury site, 1 mm, and 2 mm distal to the injury site between the two groups. However, significantly more GFP^+ axons regenerating beyond 3 mm distal to the injury site were observed in the Id2 group compared with the GFP group ($P < 0.0001$). Around 60% of axons (58.29 ± 1.15%) regenerated over 9 mm in the Id2 group, compared with less than 30% in the GFP group (25.88 ± 0.84%) (**Figure 2C**). The gastrocnemius muscle is innervated by the tibial nerve, which descends from the sciatic nerve. Two weeks after sciatic nerve crush, only a few GFP^+ fibers were found in the tibial nerve extending into gastrocnemius muscle in the GFP group (1.36 ± 0.47 axons/section). However, the number of GFP^+ fibers was significantly increased in the Id2 group (9.51 ± 0.35 axons/section, $P < 0.0001$; **Figure 3**).

Id2 facilitates reinnervation of neuromuscular junctions after sciatic nerve injury

To further investigate the promoting role of Id2 in nerve repair, α-bungarotoxin-labeled endplates inside gastrocnemius muscle were examined for neuromuscular junction (NMJ) reinnervation. As early as 2 weeks after sciatic nerve crush, a few (5–10) endplates in each gastrocnemius muscle section were found to be re-occupied by GFP^+ motor axon termini in the Id2 group, while reinnervated endplates were rarely observed in control animals at this time (**Figure 4A**). By 1 month after injury, extensive neuromuscular reinnervation had occurred in both groups. Nevertheless, the total number of re-occupied NMJs was significantly higher in the Id2 group

compared with the GFP group ($P < 0.01$; **Figure 4B** and **C**). Notably, among the reinnervated NMJs, about 85% were fully innervated in the Id2 group. However, in the GFP group, 46% of NMJs remained partially innervated 1 month after injury (**Figure 4D**).

Id2 enhances functional recovery after sciatic nerve injury

The recovery of nerve conduction and motor function was evaluated 1 month after injury. Compound muscle action potentials were recorded from gastrocnemius muscles (**Figure 5A**). The average amplitude detected from normal (uninjured) mice was 10.38 ± 0.49 mV, and the latency was 1.66 ± 0.28 ms. After sciatic nerve injury, the amplitude of compound muscle action potentials decreased and the latency was increased. Compared with the GFP group, the amplitude of compound muscle action potentials with measurements made 1 month after injury was significantly higher and the latency was shorter in the Id2 group ($P < 0.0001$; **Figure 5B** and **C**), reflecting better recovery of nerve conduction and neuromuscular transmission in the Id2 group.

CatWalk gait analysis, a tool to assess motor impairments and recovery in mice following sciatic nerve injury (Bozkurt et al., 2008; Kappos et al., 2017), was performed before injury and 1 month after injury (**Figure 6A**). Print area and stride length were decreased, while the base of support (distance between the two hind paws) was increased following sciatic nerve injury. Compared with the GFP group, animals in the Id2 group displayed better improvements in some gait parameters. Specifically, the print area of Id2 group animals was increased ($P < 0.0001$; **Figure 6B**) and the base of support was reduced to the normal level ($P < 0.0001$; **Figure 6C**). No difference in stride length was found between GFP and Id2 groups ($P > 0.05$; **Figure 6D**) after injury. These results indicate that Id2 promoted motor function recovery after sciatic nerve injury.

Discussion

Downregulation of Id2 in CNS neurons is reportedly associated with the switch of neurons from active axon growth (embryonic neurons) to a quiescent state (adult neurons) during development (Lasorella et al., 2006). Elevation of Id2 level in neurons can boost neuronal-intrinsic growth capabilities and promote axon growth. Previously, we found that Id2 showed a prominent effect on enhancing axonal growth of adult dorsal root ganglion neurons and cortical neurons *in vitro* (Yu et al., 2011; Huang et al., 2019). However, when applied *in vivo* to a spinal cord dorsal hemisection model, Id2 showed a dramatic effect on preventing axonal retraction, but only elicited very mild promotion of axonal regeneration (Yu et al., 2011). We believe this may be due to an inhibitory environment at the lesion site of the spinal cord, which prevents axonal regeneration and is unable to be overcome by Id2. Indeed, Id2 only promoted axonal growth of neurons cultured on inhibitory substrates containing axon-growth inhibitors, such as chondroitin sulfate proteoglycans and myelin-associated glycoprotein, to a small extent and failed to fully overcome these factors (Yu et al., 2011). Unlike the CNS, axons of the PNS retain considerable regenerative ability after injury, and the microenvironment of peripheral nerves is not inhibitory as is the case in injured spinal cord (Zhang et al., 2020). Therefore, we proposed that Id2 may elicit more prominent promotion of axonal regeneration after peripheral nerve injury than observed after spinal cord injury, which was confirmed in this study. We found that Id2 significantly accelerated the rate of axonal regeneration and enhanced functional recovery after sciatic nerve injury.

After peripheral nerve injury, local injury signals can rapidly turn on intrinsic programs, leading to spontaneous axonal regeneration. Many contributors to the triggering of this regenerative process have been identified, such as c-Jun (Raivich et al., 2004), activating transcription factor 3 (Seijffers et al., 2007), phosphoinositide 3-kinase-glycogen synthase kinase 3β-Smad1 (Saijilafu et al., 2013), and Lin28 (Wang et al., 2018). We previously found that Id2 expression in dorsal root ganglia becomes downregulated during development. Importantly, its expression was not upregulated after injury of the sciatic nerve (Yu et al., 2011), indicating that Id2 may not be involved in spontaneous regeneration after peripheral nerve injury. This provided us a rationale to elevate Id2 levels after peripheral nerve injury by overexpression to further enhance intrinsic growth competence.

In this study, we used intraspinal microinjection of AAV9 to deliver Id2 and GFP into motor neurons projecting to the sciatic nerve. With a universal promoter, successful gene delivery into motor neurons of adult mice and felines has been achieved by intravenous administration of self-complementary AAV9 (Duque et al., 2009). Without using a neuronal-specific promoter, here we also found that intraspinal injection of AAV9 preferentially targeted neurons. By stereotaxically microinjecting into the ventral horn of the lumbar cord, plenty of motor neurons and their axons in the sciatic nerve were labeled by GFP, enabling us to quantitatively assess axonal regeneration following sciatic nerve injury by counting GFP^+ fibers. Considering the time it takes for AAV9 expression *in vivo* and the accumulation of enough GFP signal along axons to evaluate regeneration, AAV9 was administrated before injury in this study. Further work is required to determine whether elevation of Id2 after peripheral nerve injury can also promote axonal regeneration and functional recovery. After peripheral nerve crush injury, the proximal stumps started to regenerate, while the distal stumps underwent Wallerian degeneration. The detached distal axon segments break down after injury; often, this degeneration process completes within 1 week (Gaudet et al., 2011). As the axons in our study were labeled by GFP before injury, it was difficult to clearly differentiate regenerating GFP^+ axons from the breakdown of GFP^+ axon fragments undergoing degeneration during this first week following injury. We therefore chose the time point of 2 weeks after injury for analysis of regeneration, when the degeneration process is complete.

Several potential mechanisms by which Id2 promotes axonal growth have previously been revealed in CNS neurons (Lasorella et al., 2006; Ko et al., 2016; Huang et al., 2019). As a negative regulator of basic helix-loop-helix transcriptional factors, Id2 can inhibit the transcription of their downstream gene targets, such as Nogo receptor and Sema3F, to mediate axonal growth inhibitory functions (Lasorella et al., 2006). A mechanism independent of its transcription-regulating role has also been discovered. Id2 has been found to be enriched in the growth cone of hippocampal neurons, whereby it promotes axonal growth through interaction with the actin cytoskeletal-associated protein radixin (Ko et al., 2016). We recently found in a RNA-sequencing screen that Id2 can induce the expression of Neurogenin 2 (Huang et al., 2019), a proneural gene important for driving neuronal differentiation during development (Sommer et al., 1996; Lacomme et al., 2012). More importantly, we also found that overexpression of Id2 *in vivo* by intraspinal injection of Id2 can induce Neurogenin 2 re-expression in adult neurons of the spinal cord (Huang et al., 2019). Therefore, Id2 may promote motor axon regeneration after sciatic nerve injury through these reported mechanisms.

In summary, we demonstrated here that Id2 can accelerate axonal regeneration and promote functional recovery after sciatic nerve injury in mice, which may serve as a promising target for the repair of peripheral nerve injury.

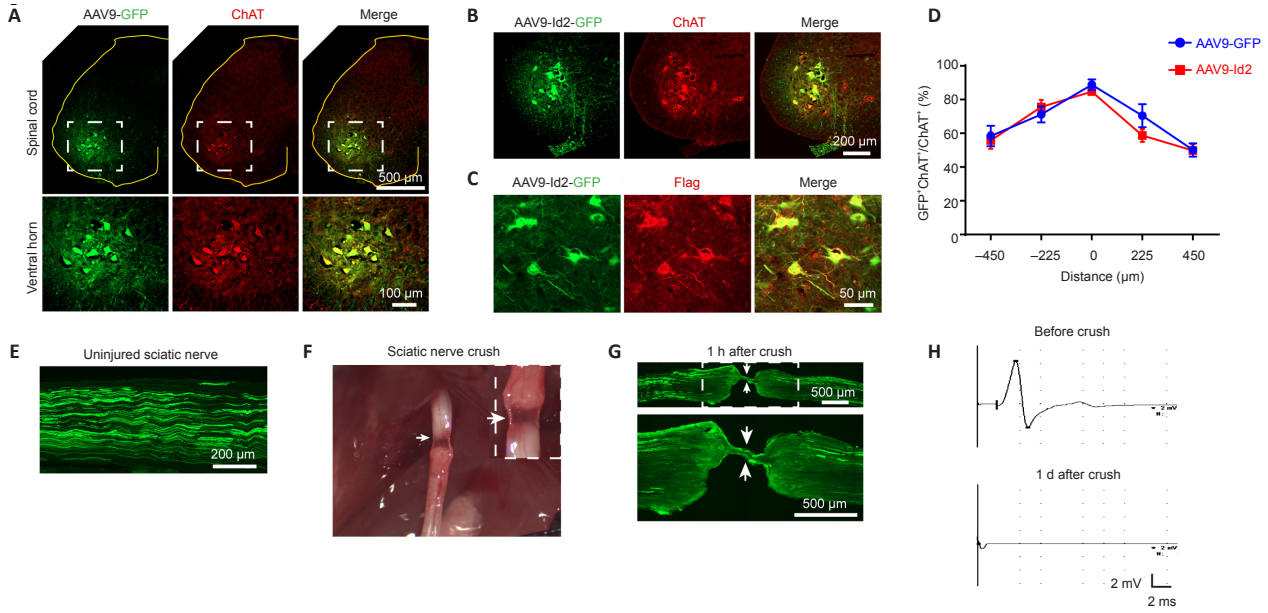

Figure 1 | Characterization of AAV9 expression and sciatic nerve injury model.
(A) Representative images from the AAV-GFP group showing GFP expression in ChAT-positive (red, Alexa Fluor 546) motor neurons located in the ventral horn of the lumbar spinal cord. Images in the bottom row show higher magnification of the dashed-line box indicating ventral horn regions of the corresponding top row. (B) Representative images from the AAV-Id2 group showing GFP expression in ChAT-positive (red) motor neurons located in the ventral horn of the spinal cord. (C) Representative images from the AAV-Id2 group showing co-expression of GFP with a Flag (red, Alexa Fluor 546) tag fused to Id2. (D) Quantification of percentages of GFP^+ motor neurons. Data are expressed as mean ± SEM (n = 5), analyzed by two-way analysis of variance followed by Bonferroni's *post hoc* test. (E) Representative image showing axons in the sciatic nerve labeled by GFP. (F) Photograph showing the sciatic nerve crush site (arrows) obtained immediately after crush injury. The crush site became transparent and nerve continuity was completely interrupted, while the epineurium of the nerve remained continuous. (G) Images of a sciatic nerve section showing complete disruption of axons while the epineurium of the nerve remained continuous in a sciatic nerve collected 1 hour after crush. (H) Electrophysiological measurement of compound motor action potentials from a gastrocnemius muscle before and after crush, following electrical stimulation of the nerve. The amplitude of compound motor action potentials disappeared 1 day after sciatic nerve crush. Scale bars are indicated in images. AAV: Adeno-associated virus; ChAT: choline acetyltransferase; GFP: green fluorescent protein; Id2: inhibitor of DNA binding 2.

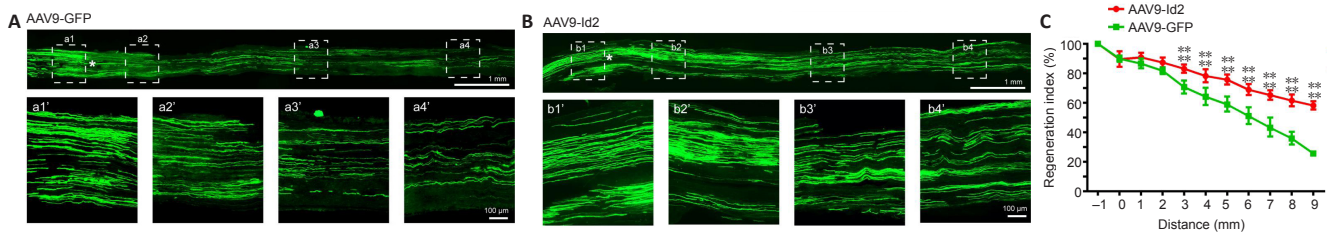

Figure 2 | Id2 promotes axonal regeneration following sciatic nerve crush.
(A, B) Representative images of GFP (A) and Id2 (B) groups showing regeneration of GFP^+ axons in the sciatic nerve collected 2 weeks after a crush injury. Asterisks indicate the site of injury. a1'–a4' in A and b1'–b4' in B are higher magnification images of the boxed regions of a1–a4 in A and b1–b4 in B, respectively. Scale bars are indicated in each row. (C) Quantification of axonal regeneration index of distal sciatic nerves. Id2 group animals displayed significantly more regenerating GFP^+ axons from 3 mm to 9 mm distal to the crush site compared with the GFP control group (****$P < 0.0001$). The regeneration index is presented as a percentage of the number of axons at each position to the number observed 1 mm proximal to the injury site. Data are expressed as mean ± SEM (n = 10 sciatic nerve samples collected from 6 mice per group, 3–5 sections from each sciatic nerve were used to calculate the regeneration index), and were analyzed by two-way analysis of variance followed by Bonferroni's *post hoc* test. AAV: Adeno-associated virus; GFP: green fluorescent protein; Id2: inhibitor of DNA binding 2.

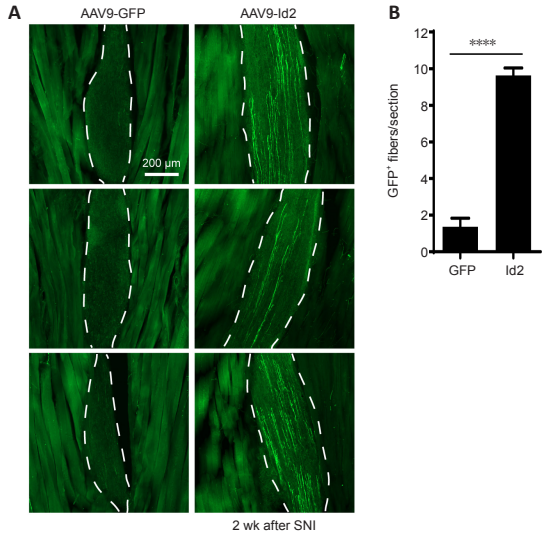

Figure 3 | Id2 accelerates regenerating axons extending into the tibial nerve branch innervating the gastrocnemius muscle.
(A) Representative images from GFP and Id2 groups to visualize GFP^+ regenerating axons in the tibial nerve (dashed outlines) projecting into the gastrocnemius muscles. Scale bar: 200 μm. (B) Quantification of numbers of GFP fibers in each section shows more GFP^+ axons present in the Id2 group compared with the GFP group (****$P < 0.0001$). Data represent mean ± SEM (n = 6 mice per group, 4–6 longitudinal gastrocnemius muscles sections per sample were counted), and were analyzed by two-tailed Student's t-test. AAV: Adeno-associated virus; GFP: green fluorescent protein; Id2: inhibitor of DNA binding 2; SNI: sciatic nerve injury.

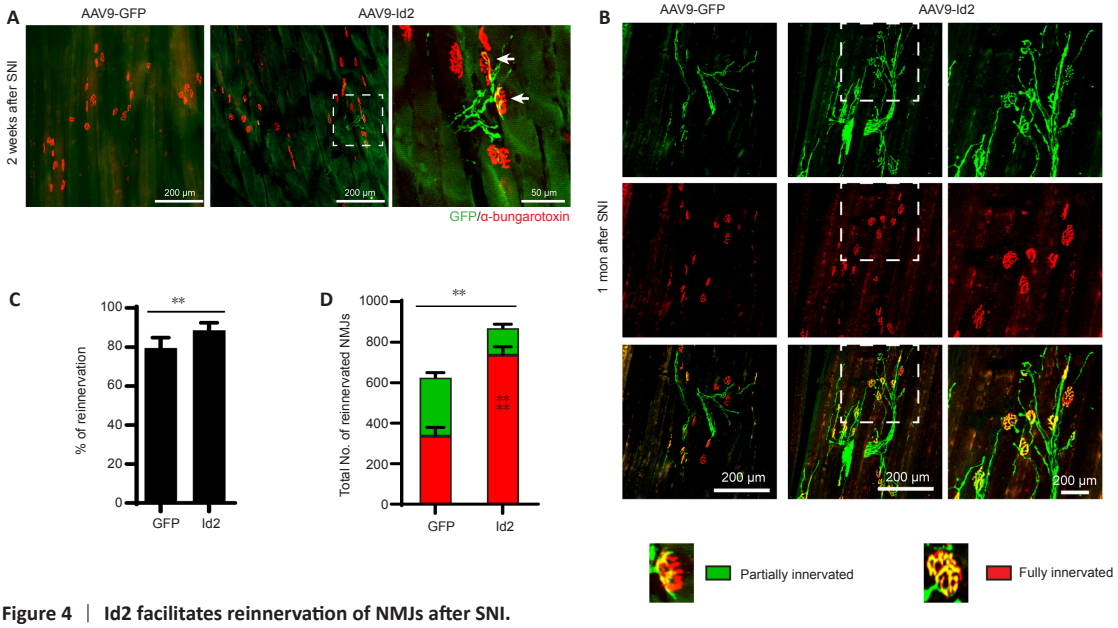

Figure 4 | Id2 facilitates reinnervation of NMJs after SNI.
(A) Representative images of NMJs labeled by α-bungarotoxin (red) and GFP (green) in the gastrocnemius muscles of GFP and Id2 groups 2 weeks after SNI. No α-bungarotoxin-labeled endplates (red) were re-occupied by GFP$^+$ axons in the GFP group 2 weeks after SNI, while a few endplates (arrows) in the Id2 group were observed to contact GFP$^+$ axons. The right image shows higher magnification of the boxed region in the middle image. (B) Representative images of NMJs in gastrocnemius muscles of GFP and Id2 groups 1 month after SNI. Right panel images are higher magnifications of the corresponding boxed regions in the middle panel. (C) Quantification of percentages of GFP$^+$ nerve-innervated endplates (**P < 0.01, *vs*. GFP group, two-tailed Student's *t*-test). (D) Quantification of numbers of NMJs fully and partially reinnervated by GFP$^+$ nerve termini (**P < 0.01, ****P < 0.0001, *vs*. GFP group, two-way analysis of variance followed by Bonferroni's *post hoc* test). Data represent mean ± SEM (n = 7; gastrocnemius muscle samples from five mice per group, one set of sections spaced 200 μm apart were counted for each muscle sample). AAV: Adeno-associated virus; GFP: green fluorescent protein; Id2: inhibitor of DNA binding 2; NMJ: neuromuscular junction; SNI: sciatic nerve injury.

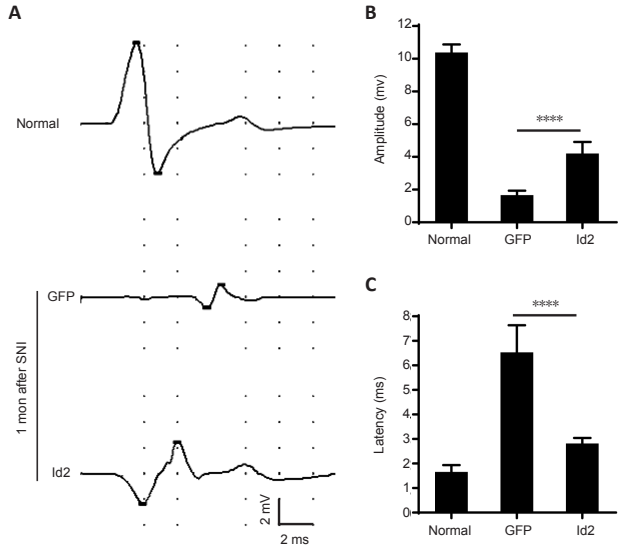

Figure 5 | Id2 enhances the recovery of nerve conduction and neuromuscular transmission following SNI.
(A) Representative compound muscle action potential of gastrocnemius muscle recorded from a normal control animal, and animals from GFP and Id2 groups 1 month after SNI. (B) Quantification shows higher amplitude in the Id2 group compared with the GFP group. (C) Quantification shows a decrease of latency in the Id2 group compared with the GFP group. Data are expressed as mean ± SD (n = 10, both sides of a total of five mice per group were recorded). ****P < 0.0001 (one-way analysis of variance followed by Turkey's *post hoc* test). AAV: Adeno-associated virus; GFP: green fluorescent protein; Id2: inhibitor of DNA binding 2; SNI: sciatic nerve injury.

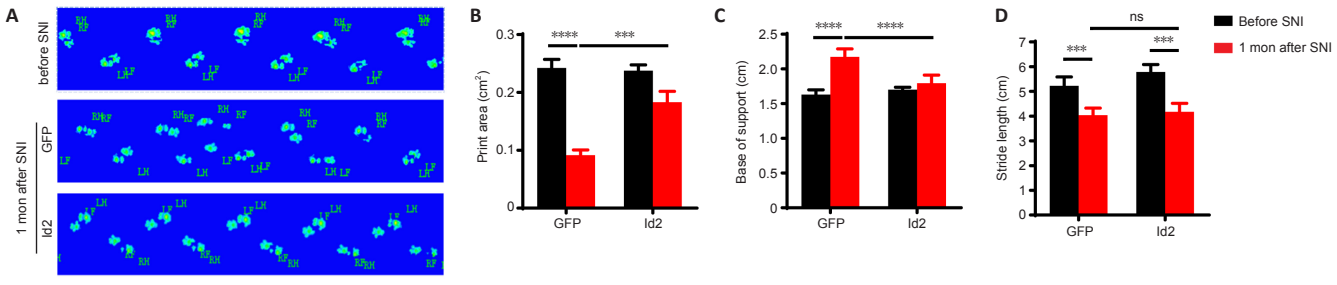

Figure 6 | Id2 improves motor function recovery after SNI.
(A) Representative photographs of walking tracks captured by the CatWalk gait analysis system before and 1 month after SNI. (B) Quantification shows the size of print area was increased in the Id2 group compared with the GFP group. (C) Quantification shows the base of support in the Id2 group was reduced compared with the GFP group. (D) Quantification shows stride length was decreased after injury, and no difference in stride length was found between GFP and Id2 groups. Data are expressed as mean ± SEM (n = 5 mice per group). ***P < 0.001, ****P < 0.0001 (two-way analysis of variance followed by Bonferroni's *post hoc* test). AAV: Adeno-associated virus; GFP: green fluorescent protein; Id2: inhibitor of DNA binding 2; LF: left front paw; LH: left hind paw; ns: not significant; RF: right front paw; RH: right hind paw; SNI: sciatic nerve injury.

Author contributions: *Study design and conception: PY and BZ; experiment implementation and data analysis: ZHH, AYF, JL, PY; technical assistance and resources: LZ; manuscript writing: PY and BZ. All authors read and approved the final manuscript.*
Conflicts of interest: *The authors declare that they have no conflict of interests.*
Financial support: *This work was supported by the National Natural Science Foundation of China, Nos. 82071369 (to PY) and 81971198 (to BZ); Guangdong grant 'Key Technologies for Treatment of Brain Disorders' of China, No. 2018B030332001 (to LZ and PY); Guangzhou Key Projects of Brain Science and Brain-Like Intelligence Technology, China, No. 20200730090 (to LZ); the Natural Science Foundation of Beijing of China, No. 7192103 (to BZ); and the Clinical Innovation Research Program of Guangzhou Regenerative Medicine and Health Guangdong Laboratory of China, No. 2018GZR0201006 (to PY). The funders had no roles in the study design, conduction of experiment, data collection and analysis, decision to publish, or preparation of the manuscript.*
Institutional review board statement: *The study was approved by the Experimental Animal Ethics Committee of Jinan University (approval No. 20160302003) on March 2, 2016.*
Copyright license agreement: *The Copyright License Agreement has been signed by all authors before publication.*
Data sharing statement: *Datasets analyzed during the current study are available from the corresponding author on reasonable request.*
Plagiarism check: *Checked twice by iThenticate.*
Peer review: *Externally peer reviewed.*

Open peer reviewers: *Katherine L Marshall, The Johns Hopkins University School of Medicine, USA; Peter Shortland, Western Sydney University, Australia; Ghasem Solgi, Hamadan University of Medical Sciences, Iran.*
Additional file: *Open peer review report 1.*

References

Benezra R, Davis RL, Lockshon D, Turner DL, Weintraub H (1990) The protein Id: a negative regulator of helix-loop-helix DNA binding proteins. Cell 61:49-59.

Bozkurt A, Deumens R, Scheffel J, O'Dey DM, Weis J, Joosten EA, Führmann T, Brook GA, Pallua N (2008) CatWalk gait analysis in assessment of functional recovery after sciatic nerve injury. J Neurosci Methods 173:91-98.

Duque S, Joussemet B, Riviere C, Marais T, Dubreil L, Douar AM, Fyfe J, Moullier P, Colle MA, Barkats M (2009) Intravenous administration of self-complementary AAV9 enables transgene delivery to adult motor neurons. Mol Ther 17:1187-1196.

Fitch MT, Silver J (2008) CNS injury, glial scars, and inflammation: Inhibitory extracellular matrices and regeneration failure. Exp Neurol 209:294-301.

Fu SY, Gordon T (1995) Contributing factors to poor functional recovery after delayed nerve repair: prolonged axotomy. J Neurosci 15:3876-3885.

Gaudet AD, Popovich PG, Ramer MS (2011) Wallerian degeneration: gaining perspective on inflammatory events after peripheral nerve injury. J Neuroinflammation 8:110.

Huang Z, Liu J, Jin J, Chen Q, Shields LBE, Zhang YP, Shields CB, Zhou L, Zhou B, Yu P (2019) Inhibitor of DNA binding 2 promotes axonal growth through upregulation of Neurogenin2. Exp Neurol 320:112966.

Huebner EA, Strittmatter SM (2009) Axon regeneration in the peripheral and central nervous systems. Results Probl Cell Differ 48:339-351.

Jiang JP, Liu XY, Zhao F, Zhu X, Li XY, Niu XG, Yao ZT, Dai C, Xu HY, Ma K, Chen XY, Zhang S (2020) Three-dimensional bioprinting collagen/silk fibroin scaffold combined with neural stem cells promotes nerve regeneration after spinal cord injury. Neural Regen Res 15:959-968.

Kappos EA, Sieber PK, Engels PE, Mariolo AV, D'Arpa S, Schaefer DJ, Kalbermatten DF (2017) Validity and reliability of the CatWalk system as a static and dynamic gait analysis tool for the assessment of functional nerve recovery in small animal models. Brain Behav 7:e00723.

Ko HR, Kwon IS, Hwang I, Jin EJ, Shin JH, Brennan-Minnella AM, Swanson R, Cho SW, Lee KH, Ahn JY (2016) Akt1-Inhibitor of DNA binding2 is essential for growth cone formation and axon growth and promotes central nervous system axon regeneration. Elife 5:e20799.

Lacomme M, Liaubet L, Pituello F, Bel-Vialar S (2012) NEUROG2 drives cell cycle exit of neuronal precursors by specifically repressing a subset of cyclins acting at the G1 and S phases of the cell cycle. Mol Cell Biol 32:2596-2607.

Lasorella A, Stegmüller J, Guardavaccaro D, Liu G, Carro MS, Rothschild G, de la Torre-Ubieta L, Pagano M, Bonni A, Iavarone A (2006) Degradation of Id2 by the anaphase-promoting complex couples cell cycle exit and axonal growth. Nature 442:471-474.

Li L, Li Y, Fan Z, Wang X, Li Z, Wen J, Deng J, Tan D, Pan M, Hu X, Zhang H, Lai M, Guo J (2019) Ascorbic acid facilitates neural regeneration after sciatic nerve crush injury. Front Cell Neurosci 13:108.

Panagopoulos GN, Megaloikonomos PD, Mavrogenis AF (2017) The present and future for peripheral nerve regeneration. Orthopedics 40:e141-156.

Raivich G, Bohatschek M, Da Costa C, Iwata O, Galiano M, Hristova M, Nateri AS, Makwana M, Riera-Sans L, Wolfer DP, Lipp HP, Aguzzi A, Wagner EF, Behrens A (2004) The AP-1 transcription factor c-Jun is required for efficient axonal regeneration. Neuron 43:57-67.

Saijilafu, Hur EM, Liu CM, Jiao Z, Xu WL, Zhou FQ (2013) PI3K-GSK3 signalling regulates mammalian axon regeneration by inducing the expression of Smad1. Nat Commun 4:2690.

Seijffers R, Mills CD, Woolf CJ (2007) ATF3 increases the intrinsic growth state of DRG neurons to enhance peripheral nerve regeneration. J Neurosci 27:7911-7920.

Sommer L, Ma Q, Anderson DJ (1996) neurogenins, a novel family of atonal-related bHLH transcription factors, are putative mammalian neuronal determination genes that reveal progenitor cell heterogeneity in the developing CNS and PNS. Mol Cell Neurosci 8:221-241.

Sulaiman W, Gordon T (2013) Neurobiology of peripheral nerve injury, regeneration, and functional recovery: from bench top research to bedside application. Ochsner J 13:100-108.

Tang BL (2020) Axon regeneration induced by environmental enrichment-epigenetic mechanisms. Neural Regen Res 15:10-15.

Toy D, Namgung U (2013) Role of glial cells in axonal regeneration. Exp Neurobiol 22:68-76.

Tzeng SF, de Vellis J (1998) Id1, Id2, and Id3 gene expression in neural cells during development. Glia 24:372-381.

Wang XW, Li Q, Liu CM, Hall PA, Jiang JJ, Katchis CD, Kang S, Dong BC, Li S, Zhou FQ (2018) Lin28 signaling supports mammalian PNS and CNS axon regeneration. Cell Rep 24:2540-2552.e6.

Wu X, Qu W, Bakare AA, Zhang YP, Fry CME, Shields LBE, Shields CB, Xu XM (2019) A laser-guided spinal cord displacement injury in adult mice. J Neurotrauma 36:460-468.

Yiu G, He Z (2006) Glial inhibition of CNS axon regeneration. Nat Rev Neurosci 7:617-627.

Yu P, Zhang YP, Shields LB, Zheng Y, Hu X, Hill R, Howard R, Gu Z, Burke DA, Whittemore SR, Xu XM, Shields CB (2011) Inhibitor of DNA binding 2 promotes sensory axonal growth after SCI. Exp Neurol 231:38-44.

Zhang L, Liu MY, Liu P, Xue X, Chen ZF, Zhang LM, Zhang J, Guo QN, Zhao JH (2020) Spinal cord homogenate promotes neurite outgrowth through activation of formyl peptide receptor 2 after spinal cord injury. Zhongguo Zuzhi Gongcheng Yanjiu Zazhi 2020:106-111.

Zhang YP, Walker MJ, Shields LB, Wang X, Walker CL, Xu XM, Shields CB (2013) Controlled cervical laceration injury in mice. J Vis Exp:e50030.

Zhou B, Yu P, Lin MY, Sun T, Chen Y, Sheng ZH (2016) Facilitation of axon regeneration by enhancing mitochondrial transport and rescuing energy deficits. J Cell Biol 214:103-119.

P-Reviewers: Marshall KL, Shortland P, Solgi G; C-Editor: Zhao M; S-Editors: Yu J, Li CH; L-Editors: Deusen VA, Yu J, Song LP; T-Editor: Jia Y